HHS Public Access

Author manuscript

Magn Reson Med. Author manuscript; available in PMC 2021 October 01.

Published in final edited form as:

Magn Reson Med. 2020 October ; 84(4): 1909–1918. doi:10.1002/mrm.28253.

Improved Velocity-Selective Labeling Pulses for Myocardial ASL

Vanessa Landes[1,*], **Ahsan Javed**[2], **Terrence Jao**[3], **Qin Qin**[4,5], **Krishna Nayak**[1,2]

[1]Department of Biomedical Engineering, Viterbi School of Engineering, University of Southern California, Los Angles, California, USA.

[2]Ming Hsieh Department of Electrical and Computer Engineering, Viterbi School of Engineering, University of Southern California, Los Angles, California, USA

[3]Keck School of Medicine, University of Southern California, Los Angles, California, USA

[4]The Russell H. Morgan Department of Radiology and Radiological Science, Division of MR Research, John Hopkins University School of Medicine, Baltimore, Maryland, USA

[5]F.M. Kirby Research Center for Functional Imaging, Kennedy Krieger Institute, Baltimore, Maryland, USA

Abstract

Purpose: To develop and evaluate an improved velocity-selective (VS) labeling pulse for myocardial arterial spin labeling (ASL) perfusion imaging that addresses two limitations of current pulses: 1) spurious labeling of moving myocardium and 2) low labeling efficiency.

Methods: The proposed myocardial VSASL labeling pulse is designed using a Fourier Transform based Velocity-Selective (FT-VS) labeling pulse train. The pulse utilizes bipolar velocity-encoding gradients, a 9-tap velocity-encoding envelope, and double-refocusing pulses with MLEV phase cycling. Amplitudes of the velocity-encoding envelope were optimized to minimize labeling of myocardial velocities during stable diastole (±2–3 cm/s) and maximize labeling of coronary velocities (10–130 cm/s during rest/stress or 10–70 cm/s during rest). Myocardial ASL experiments were performed in 7 healthy subjects using the previously developed VS-ASL protocol by Jao et al with the two proposed VS pulses and original VS pulse. Myocardial ASL experiments were also performed using FAIR ASL. Myocardial perfusion (MP) and physiological noise (PN) were evaluated and compared.

Results: Bloch simulations of the first and second proposed pulses show <2% labeling over ±3 cm/s and ±2 cm/s, respectively. Bloch simulations also show mean labeling efficiency of arterial blood is 1.23 over the relevant coronary arterial ranges. In-vivo VSASL experiments show the proposed pulses provided comparable measurements to FAIR ASL and reduced TSNR in 5 of 7 subjects compared to the original VS pulse.

Conclusion: We demonstrate an improved VS labeling pulse specifically for myocardial ASL perfusion imaging to reduce spurious labeling of moving myocardium and physiological noise.

[*]Corresponding Author: Vanessa Landes, 3740 McClintock Ave, EEB 400, University of Southern California, Los Angeles, CA 90089-2564, Phone: (213) 572-7827, Fax: (213) 740-465, vlandes@usc.edu.

Keywords

Velocity-selective labeling; arterial spin labeling; velocity selective ASL; myocardial perfusion; RF pulse design

INTRODUCTION

Myocardial arterial spin labeling (ASL) is a promising non-contrast technique for myocardial perfusion (MP) imaging. Myocardial ASL with flow alternating inversion recovery (FAIR) labeling produces MP measurements that are comparable to PET (1) and can detect clinically relevant changes in perfusion under Adenosine stress conditions (2). The current protocol is limited to a single mid short-axis slice of the heart. Evaluation of at least 3 short axis slices during rest and stress is recommended by the American Heart Association to diagnose coronary artery disease and inform treatment decisions (3). For multi-slice acquisitions, FAIR inversion slab thickness must be increased to encompass the larger imaging volume. The distance between the labeled edge and imaging slice will increase as slices are acquired farther from the aortic root. This results in increased sensitivity to transit delay and potential underestimation of MP (4).

Velocity-selective (VS) labeling would be desirable largely due to its insensitivity to transit delay; if a proper velocity cut-off (V_c) is chosen, the label signal comes from coronary blood flow adjacent to myocardium, reducing transit delay effects. Jao et al recently demonstrated VS-ASL with similar MP compared to FAIR at the cost of 2.8x lower temporal signal-to-noise ratio (TSNR). The demonstrated VS-ASL technique suffered from two limitations: 1) spurious labeling of moving myocardium and 2) low labeling efficiency (5). The previous pulse design used a BIR-8 module by Guo et al (6). This pulse had off-resonance robustness over ±250 Hz and B1 insensitivity over ±50% B1 scale, at the cost of decreased labeling efficiency and a wide transition bandwidth between labeled and unlabeled signal.

Fourier Transform based velocity selective (FT-VS) labeling techniques offer a plethora of options for velocity selective pulse design. FT-VS pulse design was first documented by Rochefort et al in 2005 and subsequent research improved upon this original concept (7). The Rochefort design used a series of sub-pulses and bipolar gradient pairs to encode signal in the velocity domain. The drawback of this technique is a shift in velocity profile as a function of static magnetic field inhomogeneities (off-resonance). Shin et al described how refocusing pulses reduced this shift and improved off-resonance robustness (8). Qin and Shin et al recently proposed VS pulse design with double refocused pulses and MLEV phase cycling (9) to further improve immunity to off-resonance (10). FT-VS pulse trains have been applied at 3T with saturation or inversion based labeling for quantifying cerebral blood flow (11) and cerebral blood volume (12). The drawback of these techniques are the presence of VS-stripe artifact in static tissues due to imperfect refocusing of the 0^{th} gradient moment with large B1 variation (>±20%) (13). Finally, Shin and Qin formally characterized the VS-stripe artifact, demonstrated effective suppression through alternate application of phase-shifted VS preparations along with k-space averaging (14). VS-stripe artifact is not compatible with myocardial VS-ASL because it can confound ASL signal, which is only 1–

4% of background tissue signal. VS phase cycling is an option to reduce the effects of stripe-artifact in static organs; however, it is not compatible with myocardial ASL because the heart moves between pairs of control and label acquisitions, compromising the effectiveness of the averaging step. Although an ideal FT-VS pulse design does not currently exist for myocardial ASL, these FT-VS design techniques can be explored and tailored for this specific application.

An ideal FT-VS pulse for myocardial ASL would include 1) inversion over a short duration to increase labeling efficiency, 2) refocusing pulses with MLEV phase cycling to reduce sensitivity to off-resonance, 3) labeling of flowing blood only to maintain compatibility with background suppression, and 4) bipolar velocity-encoding gradients to remove the influence of VS-stripe artifact on ASL signal. In this manuscript, we utilize FT-VS pulse design concepts to produce pulses specifically for myocardial ASL at 3T that reduce spurious labeling of moving myocardium and improve labeling efficiency. ASL measurements and physiological noise are compared in 1) the original implementation of VSASL (5), 2) an implementations of VSASL using proposed pulses, and 3) FAIR-ASL (15).

METHODS

Phantom and in-vivo experiments were performed on a 3T whole body scanner (Signa HDxT; General Electric Healthcare, Waukesha, WI) using an 8-channel cardiac coil receiver array.

VS pulse design

The original VS pulse (VS-Orig) used by Jao et al (5) utilized an adiabatic symmetric BIR-8 pulse design (6). This pulse was optimized for off-resonance and B1 conditions in the heart and had the following parameters: sub-pulse duration = 2.24 ms, $\kappa = 62.96$, $\omega_{max} = 21.6$, and $\xi = 20.5$. Bipolar gradients were inserted between the paired refocusing pulses to avoid the striping artifact in label acquisitions (14,16), and no gradients were used in control acquisitions, imparting T_2-weighting only. Laminar flow was assumed, with uniform velocity distribution from 0 to twice the mean velocity within each blood vessel. Under this assumption, the excitation profile became a sinc-shaped function of the mean velocity, and Vc was defined as the first zero-crossing of the velocity profile. $V_c = 10$ cm/s with velocity-encoding along the through-slice direction gave the best performance in a previous study (5) and was used in this study.

The design of the proposed VS pulses (VS-Prop) was informed by physiologic velocity ranges for myocardium and coronary blood during mid-diastole, the cardiac phase when VS labeling was applied. The design did not assume laminar flow. During mid-diastole, coronary blood velocities are highest and myocardial motion is lowest. Literature suggests that myocardial through-plane velocities within a range of ±3 cm/s during diastole (17,18). Gorcsan et al reported a range of peak myocardial velocities along the endocardial walls in healthy subjects and heart disease patients using tissue Doppler imaging (13). From early to late diastole, the velocity range was 2.90±0.14 cm/s to 1.15±0.74 cm/s in posterior segments, and 2.36±0.69 cm/s to 1.94±0.88 cm/s in anteroseptal segments (17). Movement was less in abnormal segments of heart disease patients; from early to late diastole, the

velocity range was 1.4±0.7 cm/s to 0.7±0.3 cm/s in posterior segments and was 1.83±0.84 to 0.96±0.53 cm/s in anteroseptal segments. Simpson et al reported a mean peak longitudinal velocity (motion towards the apex) of −6.5 ± 1.85 cm/s in the mid-short axis of the heart during early diastole in healthy subjects using phase-velocity mapping, an MRI-based myocardial velocity mapping technique, but was within a range of ±3 cm/s from mid-diastasis to early systole (18). As previously noted by Jao et al., a VS pulse that labels low velocities can result in inadvertent labeling of myocardium, substantially increasing physiological noise (5). The ideal VS pulse will therefore be played during mid-diastasis and label nothing between ±3 cm/s, while maximally labeling coronary blood.

Coronary arterial velocities vary between different arteries and between different disease states. In general, proximal coronary velocities are higher than the distal velocities, and the velocities in the left anterior descending (LAD) artery are higher than in the left circumflex (LCX) and right coronary artery (RCA) (19). Peak coronary velocities in healthy individuals and coronary artery disease (CAD) patients were reported using Doppler Flow wires, and ranged from 49±20 cm/s in the proximal LAD to 28±8 cm/s in the distal RCA (19–21). Peak coronary velocities in healthy individuals with adenosine stress were reported from 104±28 cm/s in the proximal LAD and 67±16 cm/s in the distal RCA (19). The coronary vasodilator reserve, the ratio of stress to rest mean velocity, was 2.3 ± 0.8 in healthy arteries and was 1.6 ± 0.7 in diseased arteries, indicating a reduced stress response in diseased arteries (19).

In this work, velocity was encoded in the base-apex direction, resulting in potential angle effects. This means pulses were sensitive to velocity along a single direction, and the encoding velocity was the actual velocity multiplied by the cosine of the angle between the vessel and the direction of velocity encoding (22). In this work, we accounted for angles of up to 60º. We designed pulses to label spins within a velocity range, where the lowest velocity is ½, or cos(60°), of the mean minus one standard deviation of the coronary velocity in the distal RCA. The upper velocity is the mean plus one standard deviation of the coronary velocity in the proximal LAD. The relevant coronary arterial velocity range for subjects at rest then became 10–70 cm/s along the base-apex direction. This range increased to 10–130 cm/s when considering both rest and stress conditions.

Pulse design must also consider imaging imperfections. In cardiac MRI at 3 Tesla, the amplitude of the transmitted RF field (B1) field varies by up to 50% across the myocardium, with a decreasing B1 scale from the lateral to septal wall (23). There is also substantial off-resonance due to proximity of the lungs and draining veins. The reported variation is 125±40.6 Hz across the entire heart at 3T (23,24). This necessitates the need for a VS pulse which is robust to both B1 and off-resonance variation. In this work, we considered the relevant B1 scale (b_1) to be 0.5 to 1 and the relevant off-resonance range to be ±125 Hz. Note that both b_1 and off-resonance variation increase with static magnetic field strength. This work was performed at 3T, but we would expect these constraints to be relaxed at ≤1.5T (24) and more stringent at ≥7T (25).

The proposed VS pulse was based on designs by Shin et al and Qin et al, due to their robustness to off-resonance and B1 variation (8,10), as well as their ability to predictably modify the velocity profile using FT-VS encoding techniques. 9 sub-pulses were used with

double-refocusing and MLEV-16 phase cycling (9). The velocity-encoding gradients were adjusted to include only bipolar gradient pairs between the paired refocusing pulses, which eliminated the potential for VS-stripe artifact (14,16). Control acquisitions were similar to label acquisitions, except gradients were turned off. Velocity field of view (FOV_v) was chosen to be twice the mean relevant coronary velocity range. Initial values for the 9 sub-pulse amplitudes were designed using the RF Tools toolbox (26). Specifically, we used a linear-phase inversion design with a time-bandwidth product of 6, assuming no relaxation, off-resonance, or B1 effects. This initial design was empirically chosen for its ability to minimize labeling between ±3 cm/s, the range of myocardial motion during stable diastole, while maximizing labeling between the relevant coronary range. π phase was added to alternate sub-pulse amplitudes to shift FOV_v and invert signal in coronary velocities as opposed to static tissues. This allows for compatibility with background suppression designed for the original VSASL scheme.

Sub-pulse amplitudes p were optimized to maximize coronary ASL signal and minimize labeling of myocardium over a set of values $\mathbf{\Phi} = (v; \Delta f; b_1)$, with velocities $v = -0.5FOV_v:0.5:0.5FOV_v$ cm/s, off-resonance values Δf=−125:25:125 Hz, and B1 scale values b_1 = 0.5:0.1:1.0. ASL signal $S(\mathbf{\Phi}, p)$ was defined as the difference between Bloch simulations of magnetization immediately after the control pulse and after the label pulse (27). Simulations assumed no relaxation. The cost function, below, was adjusted for two separate settings of myocardial and coronary velocities: 1) $|v| \leq 3$cm/s and $10 \leq |v| \leq 130$ cm/s, and 2) $|v| \leq 2$ cm/s and $10 \leq |v| \leq 70$ cm/s, respectively. The first setting was chosen to cover the complete range of velocities found in literature at rest and stress for subjects, while the second setting was chosen in an effort to maximize ASL signal from coronary arterial blood in healthy subjects at rest at the cost of relaxing the assumption for a relevant myocardial velocity range. These two terms were weighted using parameter λ. The cost function was then

$$p = \text{argmin}_p \left\{ -\underset{\mathbf{\Phi} \in \mathbf{\Phi}_b}{\text{mean}} |S(\mathbf{\Phi}, p)| + \lambda \underset{\mathbf{\Phi} \in \mathbf{\Phi}_m}{\max} |S(\mathbf{\Phi}, p)| \right\},$$

$\mathbf{\Phi}_b$ was the set of $\mathbf{\Phi}$ that includes velocities for coronary arterial blood, and $\mathbf{\Phi}_m$ was the set of $\mathbf{\Phi}$ that includes velocities for myocardial movement during stable diastole. $\mathbf{\Phi}$ is depicted in Figure 1.

λ allowed a tradeoff between maximizing ASL signal from coronary blood flow against suppression of spurious myocardial signal (higher values suppress spurious myocardial signal, while lower values maximize ASL signal from coronary blood flow). Sub-pulse amplitudes were optimized using different values of λ (0.001, 0.01, 0.1, 1, 10, 100, and 1000) to assess the relative importance of weighting myocardial labeling compared to coronary blood labeling. The final λ was chosen as the highest λ where $\underset{\mathbf{\Phi} \in \mathbf{\Phi}_m}{\max} |S(\mathbf{\Phi}, p)| < 0.02$ to allow a low tolerance for potential spurious labeling of myocardium while maximizing labeling of coronary blood. Maximum labeling of moving myocardium and

mean coronary velocity labeling can be seen as a function of λ in Supporting Information Figure S1. FT-VS pulse design source code and demo scripts are available (https://github.com/usc-mrel/velocity_demo) to facilitate FT-VS pulse designs for other applications.

Bloch Simulations

Bloch simulations were obtained of the longitudinal magnetization after the VS-Prop pulses using MATLAB (MathWorks, Inc., Natick, MA) over $v = \pm FOV_v$, $b_1 = 0.5–1$, and $\Delta f = \pm 125$ Hz to observe pulse performance in conditions expected in the heart at 3T, before and after optimization of sub-pulse amplitudes. In addition, the k_v-encoding location was calculated during each velocity-encoding sub-pulse and was compared to the $\Delta f = 0$, $b_1 = 1$ VS profile before and after optimization.

Silicone Phantom Experiments

Experiments were performed in a silicone oil phantom (T_1/T_2 = 1111/227 ms) in order to determine the proper delay after each bipolar gradient pair and mitigate artifacts from gradient imperfections. Silicone oil is a suitable substance for evaluating these types of artifacts due to its low diffusion coefficient and long relaxation times (6,11). A time delay was empirically chosen by gradually increasing the time delay and evaluating signal difference between center-out GRE images acquired immediately after the VS-Prop pulse with FOV_v = 80 cm/s. This pulse was used because it had larger gradients than the VS-Prop pulse with FOV_v = 140 cm/s and was expected to incur larger artifacts. A final delay time was chosen based on the shortest delay with minimal difference signal.

ASL signal was evaluated to determine potential signal bias by acquiring center-out GRE images (matrix size=96×96, FOV=20 cm, slice thickness=1 cm) without a pre-pulse, immediately after a VS-label pulse, and immediately after VS-control pulse. The difference between label and control images was taken and divided by a center-out GRE image. An ROI was drawn around the phantom. Mean, min, max, and standard deviation were calculated over the ROI.

ASL experiments

7 healthy volunteers (3M/4F, age 24–33Y) were scanned in the study and all procedures were conducted in accordance with protocols approved by Internal Review Board of the University of Southern California. The VS-BGS scheme described by Jao et al (5) was used with the 1) VS-Orig, 2) VS-Prop (FOV_v = 140 cm/s), and 3) VS-Prop (FOV_v = 80 cm/s). The FAIR-ASL described by Zun et al was also used (4). Image acquisition was performed in a single mid short-axis slice using a snapshot 2DFT balanced SSFP sequence (TR=3.2ms, TE=1.5ms, prescribed FA=50°, matrix size=96×96, FOV=18–22 cm, slice thickness=10 cm, GRAPPA (auto-calibration signal lines=24, acceleration factor=1.6). Semi-automatic segmentation of the myocardium was performed (28). For VS-BGS ASL experiments, the timing of the background suppression pulse was optimized for different heart rates and took into account T_2 signal loss from the respective VS labeling pulses (5,29). Pre-scan was run before ASL experiments in each subject, and not in between, to help ensure comparable scanner settings between experiments.

As noted by Jao et al (5) and Zun et al (4), six pairs of control and labeled images were acquired for myocardial perfusion (MP), physiological noise (PN), and temporal signal-to-noise ratio (TSNR) measurements. Each image pair was acquired with breath holding (10–12 s) to prevent misregistration and to avoid spurious labeling from respiratory motion. A 6-s delay between image acquisition allowed full recovery between labeling and imaging. In an additional 2-s breath hold, a baseline image was acquired without labeling to calculate coil sensitivity maps and a noise image was acquired to calculate the noise covariance matrix. MP, PN, and TSNR were calculated globally across the mid-short axis slice of the heart in each ASL experiment. VS-ASL calculations were performed as described previously (5), except that the VS-prop signal was divided by 2 to account for an inversion of flowing spins and the T_2-weighting term was updated to reflect the duration of the VS-Prop pulses. FAIR-ASL calculations were performed as described by Zun et al (4). A two one-sided test, or TOST test, was used to evaluate equivalence of MP values between methods. A t-test was performed to determine whether TSNR was different between methods.

RESULTS

Figure 2 illustrates the proposed pulse (FOV_v = 140 cm/s). It has a pulse duration of 74 ms, which includes a 0.25 ms delay after each gradient pair to reduce sensitivity to gradient imperfections. These imperfections include eddy currents and are scanner-specific. We found a delay of 0.25 ms to be adequate on our system. The proposed pulse is similar to the initial guess with modified sub-pulse amplitudes. Velocity-encoding sub pulses work together to shape the velocity profile, and most velocity-selective inversion of spins occurs in the middle sub-pulse of highest-amplitude.

Figure 3 illustrates the reduced labeling of myocardium and improved labeling efficiency of blood after optimization. ASL signal across myocardial velocities, reflecting potential to spuriously label moving myocardium, varied over ±2% for $v \neq 0$ cm/s. This is especially apparent as a function of off-resonance. After optimization, ASL signal across myocardial velocities is substantially reduced. ASL signal is <0.002 for $|v| \leq 2$ cm/s and up to 0.02 for $2 < v \leq 3$ cm/s.

Figure 4 demonstrates the Fourier-relationship between $\Delta f = 0$, $b_1 = 1$ velocity profile and sub-pulse envelope. It depicts k_v-encoding as a function of velocity-encoding sub-pulse amplitude and the corresponding $\Delta f = 0$, $b_1 = 1$ velocity profile, before and after optimization. The overall shape of the sub-pulses is sinc-shaped to select a range of velocities before and after optimization, and the middle sub-pulse amplitude remained. Other sub-pulse amplitudes were adjusted with optimization to improve pulse performance. The stop-band of the velocity-selective profile flattens to reduce labeling of myocardial velocities, and the pass-band ripples are reduced.

Supporting Information Figure S2 demonstrates low ASL signal bias in an oil phantom (<0.3%) due to gradient imperfections with the proposed VS pulse and a delay 0.25 ms delay after each gradient pair. This bias is on the order of noise. A shorter delay was found to increase ASL signal bias due to increased sensitivity to gradient imperfections.

Supporting Information Figure S3 demonstrates labeling at the level of the coronary arteries. Center-out GRE images of the cross-section of the right coronary artery were obtained 1) immediately after a VS label acquisition, and 2) immediately after a VS control acquisition. A clear difference is seen between control and label coronary blood signal.

Supporting Information Figure S4 presents examples of control and label acquisitions in the VS-Orig and VS-Prop pulse. It illustrates the expected T_2-weighting in control images and labeling of blood signal in label images. Furthermore, these images demonstrate reduced labeling of left ventricular blood pool signal in the VS-Prop pulse compared to the VS-Orig pulse. The VS-Prop pulse is designed to label coronary velocities; velocities in the left ventricular blood pool are often much higher.

Figure 5 shows MP and PN measured using 4 ASL experiments (three VS and one FAIR) across 7 subjects. MP is within a physiologically reasonable range (1–3 ml/g/min). TOST with a difference of 0.5 ml/g/min and p=0.05 indicated MP measured with FAIR-ASL and VS-Prop VS-ASL (FOV_v=140 cm/s) were statistically comparable, while MP measured with FAIR-ASL and VS-Orig VS-ASL were not comparable. A t-test indicated FAIR-ASL and VS-Prop VS-ASL did not have significantly higher TSNR compared to VS-Orig VS-ASL (p=0.07).

Figure 6 depicts a reduction in spurious labeling of moving myocardium in the VS-Prop pulse compared to the VS-Orig pulse. The VS-Orig pulse shows a high MP measurement of >4 ml/g/min in the lateral wall, which is likely due to spuriously labeled myocardium. MP is more uniform across the myocardium using the VS-Prop pulse, suggesting a reduction in spurious labeling.

DISCUSSION

The specially tailored VS pulse was demonstrated to reduce spurious labeling of moving myocardium and reduce PN compared to the prior implementation of myocardial VSASL. The new VSASL scheme also gave statistically equivalent MP compared to FAIR ASL, as expected. It is anticipated that this VS pulse will be useful for VSASL with reduced sensitivity to transit delay.

This work demonstrates how FT-based velocity-selective RF pulses can be tailored for a specific application. Low-field applications and brain applications will likely require optimization over smaller range of off-resonance and B1 variations. It is possible that single or no inversions will be required between velocity encoding sub-pulses. This will allow for a sufficient, shorter pulse to be designed. Applications in other areas of the body will also change pulse design criteria. Body applications with less motion will relax constraints on the stopband of the designed velocity selective pulse. This tradeoff could allow for a pulse design with higher labeling efficiency across the desired range of velocities. Other VS applications may also benefit from consideration of relaxation effects. The sub-pulse amplitudes of the velocity selective inversion pulses were optimized assuming no T_2 relaxation, which simplified the optimization problem. Empirically, we found that optimizing using T_2 relaxation for arterial blood, myocardium, or a combination of both

with respect to their velocities resulted in similar sub-pulse amplitudes. However, it can be desirable to consider relaxation in other VS applications.

It should be noted that there is potential for improvement even in the prosed FV-VS pulses for myocardial ASL. FT-VS pulse designs could further benefit from a systematic analysis on the effects of different initial parameters on optimization procedures. In addition, we observed that the first sub-pulse amplitude was near-zero suggesting that the proposed FT-VS pulse could be truncated from the beginning to right before the second sub-pulse to reduce pulse duration with minimal impact on velocity selection (30).

The proposed VS pulses can easily be modified for compatibility with steady-pulsed ASL (SPASL) techniques. SPASL is desirable for its ability to efficiently acquire perfusion signal by driving the tissue magnetization into a perfusion-dependent steady-state (31). A SPASL-compatible VS pulse can be designed by adjusting the velocity-encoding sub-pulses to achieve velocity-selective saturation instead of inversion.

A tradeoff existed between labeling efficiency and potential to spuriously label myocardium in the two proposed VS pulses. VS-Prop (FOV_v=140 cm/s) was designed to label coronary velocities at rest and stress. Bloch simulations demonstrated less spurious labeling but lower labeling efficiency. VS-Prop (FOV_v=80 cm/s) was designed to label coronary velocities only at rest and Bloch simulations demonstrated increased potential for spurious labeling for v>2 cm/s but higher labeling efficiency. This study showed potential comparability between the two VS-Prop pulses (FOV_v=80 and 140 cm/s), however it only considered healthy subjects at rest. A future study is needed to demonstrate differences under stress.

Statistical testing in this study is limited by analysis across 7 subjects. MP measurements across methods presented in this paper were physiologically reasonable and statistically equivalent using FAIR ASL and VS-Prop VSASL. TSNR measured with VS-Prop VSASL and FAIR ASL were statistically higher compared to the original VS-Orig VSASL across the 7 subjects, as expected. It should be noted that it was not higher in every subject. This could be due to lack of spurious labeling using VS-Orig VSASL, or other physiological factors.

Labeling of coronary velocities was demonstrated with each VS pulse in this paper but did not result in reasonable quantitative measurements of labeling efficiency. It was expected that coronary blood flow would be inverted in the proposed VS pulses and saturated in the original VS pulse, however it was difficult to confirm this expectation and measurements were not reliable due to practical limitations. For example, insufficient resolution can cause partial voluming to affect measurements. In addition, Bloch simulations demonstrated how coronary labeling efficiency varies as a function of off-resonance and B1.

This study, like the previous study of myocardial VSASL (5), lacks experimental verification of insensitivity to transit delay. VSASL in the brain is traditionally done with a low V_c to label blood at the capillary level and eliminate transit delay effects (6,11). This is experimentally demonstrated by evaluating ASL signal at several post-labeling delays, and fitting with a kinetic model. Myocardial VSASL is performed with a higher V_c to avoid spurious labeling of myocardium. Theoretically, the proposed VS pulses are designed to

label coronary blood and reduce transit delay effects. In reality, coronary blood flow may be labeled but the extent to which transit delay is reduced is unknown due to a higher V_C causing blood to be labeled at higher levels of coronary vasculature depending on an individual's particular anatomy. Future work is needed to experimentally verify the insensitivity to transit delay. This is complicated to perform in the heart since coronary flow is pulsatile, labeling and imaging must be cardiac gated, and short post-labeling delays are very difficult to acquire. Validation could instead be performed by comparing the performance of VS labeling and FAIR labeling in multi-slice experiments. Sensitivity to transit delay is increased with multi-slice FAIR due to the need for a thicker inversion slab. Validation could also be performed in subjects with slow coronary flow or substantial collaterals, although identification of such a cohort could be challenging.

CONCLUSION

We have demonstrated reduced physiological noise in myocardial VSASL with specially tailored velocity-selective inversion pulse. The proposed VS pulse was designed using a Fourier Transform based Velocity-Selective labeling pulse train and was optimized to reduce spurious labeling of moving myocardium and maximize labeling of coronary blood velocities in the cardiac 3T MRI environment. This technique gives comparable MP measurements as FAIR ASL, making it a suitable candidate for multislice myocardial ASL and for myocardial ASL in patients with slow coronary flow.

Supplementary Material

Refer to Web version on PubMed Central for supplementary material.

ACKNOWLEDGEMENTS

We thank Jia Guo and Eric Wong for helpful discussions. We gratefully acknowledge funding from the National Institutes of Health (R01-HL130494, PI: Nayak)

A preliminary version of this work was presented at ISMRM 2019 (Abstract #4967) and was submitted to this journal (MRM-19–20585 and MRM-19_20585.R1).

References

1. Chareonthaitawee P, Kaufmann PA, Rimoldi O, Camici PG. Heterogeneity of resting and hyperemic myocardial blood flow in healthy humans. Cardiovasc. Res. 2001;50:151–161. doi: 10.1016/S0008-6363(01)00202-4. [PubMed: 11282088]
2. Zun Z, Varadarajan P, Pai RG, Wong EC, Nayak KS. Arterial spin labeled CMR detects clinically relevant increase in myocardial blood flow with vasodilation. JACC Cardiovasc. Imaging 2011;4:1253–1261. doi: 10.1016/j.jcmg.2011.06.023. [PubMed: 22172781]
3. Cerqueira MD. Standardized Myocardial Segmentation and Nomenclature for Tomographic Imaging of the Heart. Child. A Glob. J. Child Res. 2003:1448–1453. doi: 10.1161/01.CIR.0000060923.07573.F2.
4. Zun Z, Wong EC, Nayak KS. Assessment of myocardial blood flow (MBF) in humans using arterial spin labeling (ASL): feasibility and noise analysis. Magn. Reson. Med. 2009;62:975–983. doi: 10.1002/mrm.22088. [PubMed: 19672944]
5. Jao TR, Nayak KS. Demonstration of velocity selective myocardial arterial spin labeling perfusion imaging in humans. Magn. Reson. Med. 2018;80:272–278. doi: 10.1002/mrm.26994. [PubMed: 29106745]

6. Guo J, Meakin JA, Jezzard P, Wong EC. An optimized design to reduce eddy current sensitivity in velocity-selective arterial spin labeling using symmetric BIR-8 pulses. Magn. Reson. Med. 2015;73:1085–1094. doi: 10.1002/mrm.25227. [PubMed: 24710761]
7. De Rochefort L, Maître X, Bittoun J, Durand E. Velocity-selective RF pulses in MRI. Magn. Reson. Med. 2006;55:171–176. doi: 10.1002/mrm.20751. [PubMed: 16342055]
8. Shin T, Hu BS, Nishimura DG. Off-resonance-robust velocity-selective magnetization preparation for non-contrast-enhanced peripheral MR angiography. Magn. Reson. Med. 2013;70:1229–1240. doi: 10.1002/mrm.24561. [PubMed: 23192893]
9. Levitt M Broadband Heteronuclear Decoupling. J. Magn. Reson. 1981;47:328–330. doi: 10.1016/0022-2364(82)90124-X.
10. Qin Q, Shin T, Schar M, Guo H, Chen H, Qiao Y. Velocity-selective magnetization-prepared non-contrast-enhanced cerebral MR angiography at 3 Tesla: Improved immunity to B0/B1 inhomogeneity. Magn. Reson. Med. 2016;75:1232–1241. doi: 10.1002/mrm.25764. [PubMed: 25940706]
11. Qin Q, van Zijl PCM. Velocity-selective-inversion prepared arterial spin labeling. Magn. Reson. Med. 2016;76:1136–1148. doi: 10.1002/mrm.26010. [PubMed: 26507471]
12. Qin Q, Qu Y, Li W, Liu D, T S, Y Z, Lin D, van Zijl P, Wen Z. Cerebral blood volume mapping using Fourier-transform-based velocity-selective saturation pulse trains. Magn. Reson. Med. 2019;81:3544–3554. doi: 10.1002/mrm.27668. [PubMed: 30737847]
13. Shin T, Qin Q, Park JY, Crawford RS, Rajagopalan S. Identification and reduction of image artifacts in non–contrast-enhanced velocity-selective peripheral angiography at 3T. Magn. Reson. Med. 2016;76:466–477. doi: 10.1002/mrm.25870. [PubMed: 26308243]
14. Shin T, Qin Q. Characterization and suppression of stripe artifact in velocity-selective magnetization-prepared unenhanced MR angiography. Magn. Reson. Med. 2018;80:1997–2005. doi: 10.1002/mrm.27160. [PubMed: 29536569]
15. Zun Z, Wong EC, Nayak KS. Assessment of myocardial blood flow (MBF) in humans using arterial spin labeling (ASL): feasibility and noise analysis. Magn. Reson. Med. 2009;62:975–983. doi: 10.1002/mrm.22088. [PubMed: 19672944]
16. Fan Z, Sheehan J, Bi X, Liu X, Carr J, Li D. 3D noncontrast MR angiography of the distal lower extremities using flow-sensitive dephasing (FSD)-prepared balanced SSFP. Magn. Reson. Med. 2009;62:1523–1532. doi: 10.1002/mrm.22142. [PubMed: 19877278]
17. Gorcsan J, Gulati VK, Mandarino WA, Katz WE. Color-coded measures of myocardial velocity throughout the cardiac cycle by tissue Doppler imaging to quantify regional left ventricular function. Am. Heart J. 1996;131:1203–1213. doi: 10.1016/S0002-8703(96)90097-6. [PubMed: 8644601]
18. Simpson R, Keegan J, Firmin D. Efficient and reproducible high resolution spiral myocardial phase velocity mapping of the entire cardiac cycle. J. Cardiovasc. Magn. Reson. 2013;15:1–14. doi: 10.1186/1532-429X-15-34. [PubMed: 23324167]
19. Ofili EO, Labovitz AJ, Kern MJ. Coronary flow velocity dynamics in normal and diseased arteries. Am. J. Cardiol. 1993;71. doi: 10.1016/0002-9149(93)90128-Y.
20. Pereira VFA, De Carvalho Frimm C, Rodrigues ACT, Tsutsui JM, Cúri M, Mady C, Ramires JAF. Coronary flow velocity reserve in hypertensive patients with left ventricular systolic dysfunction. Clin. Cardiol. 2002;25:95–102. doi: 10.1002/clc.4960250304. [PubMed: 11890376]
21. Anderson HV, Stokes MJ, Leon M, Abu-Halawa SA, Stuart Y, Kirkeeide RL. Coronary artery flow velocity is related to lumen area and regional left ventricular mass. Circulation 2000;102:48–54. doi: 10.1161/01.CIR.102.1.48. [PubMed: 10880414]
22. Wong EC, Cronin M, Wu W-C, Inglis B, Frank LR, Liu TT. Velocity-selective arterial spin labeling. Magn. Reson. Med. 2006;55:1334–1341. doi: 10.1002/mrm.20906. [PubMed: 16700025]
23. Sung K, Nayak KS. Measurement and characterization of RF nonuniformity over the heart at 3T using body coil transmission. J. Magn. Reson. Imaging 2008;27:643–648. doi: 10.1002/jmri.21253. [PubMed: 18306272]
24. Kellman P, Herzka DA, Arai AE, Hansen MS. Influence of Off-resonance in myocardial T1-mapping using SSFP based MOLLI method. J. Cardiovasc. Magn. Reson. 2013;15:1–8. doi: 10.1186/1532-429X-15-63. [PubMed: 23324167]

25. Niendorf T, Sodickson DK, Krombach GA, Schulz-Menger J. Toward cardiovascular MRI at 7 T: Clinical needs, technical solutions and research promises. Eur. Radiol. 2010;20:2806–2816. doi: 10.1007/s00330-010-1902-8. [PubMed: 20676653]

26. Pauly J, Nishimura D, Macovski A, Roux P Le. Parameter Relations for the Shinnar-Le Roux Selective Excitation Pulse Design Algorithm. IEEE Trans. Med. Imaging 1991. doi: 10.1109/42.75611.

27. Hargreaves B Bloch Simulation Equation. mrsrl.stanford.edu/~brian/bloch/.

28. Javed A, Jao TR, Nayak KS. Motion correction facilitates the automation of cardiac ASL perfusion imaging. J. Cardiovasc. Magn. Reson. 2015;17:P51. doi: 10.1186/1532-429x-17-s1-p51.

29. Maleki N, Dai W, Alsop DC. Optimization of background suppression for arterial spin labeling perfusion imaging. Magn. Reson. Mater. Physics, Biol. Med. 2012;25:127–133. doi: 10.1007/s10334-011-0286-3.

30. Matson GB. Design strategies for improved velocity-selective pulse sequences. Magn. Reson. Imaging. 2017;44:146–156. doi: 10.1016/j.mri.2017.09.006. [PubMed: 28890384]

31. Capron T, Troalen T, Robert B, Jacquier A, Bernard M, Kober F. Myocardial perfusion assessment in humans using steady-pulsed arterial spin labeling. Magn. Reson. Med. 2015;74:990–998. doi: 10.1002/mrm.25479. [PubMed: 25263761]

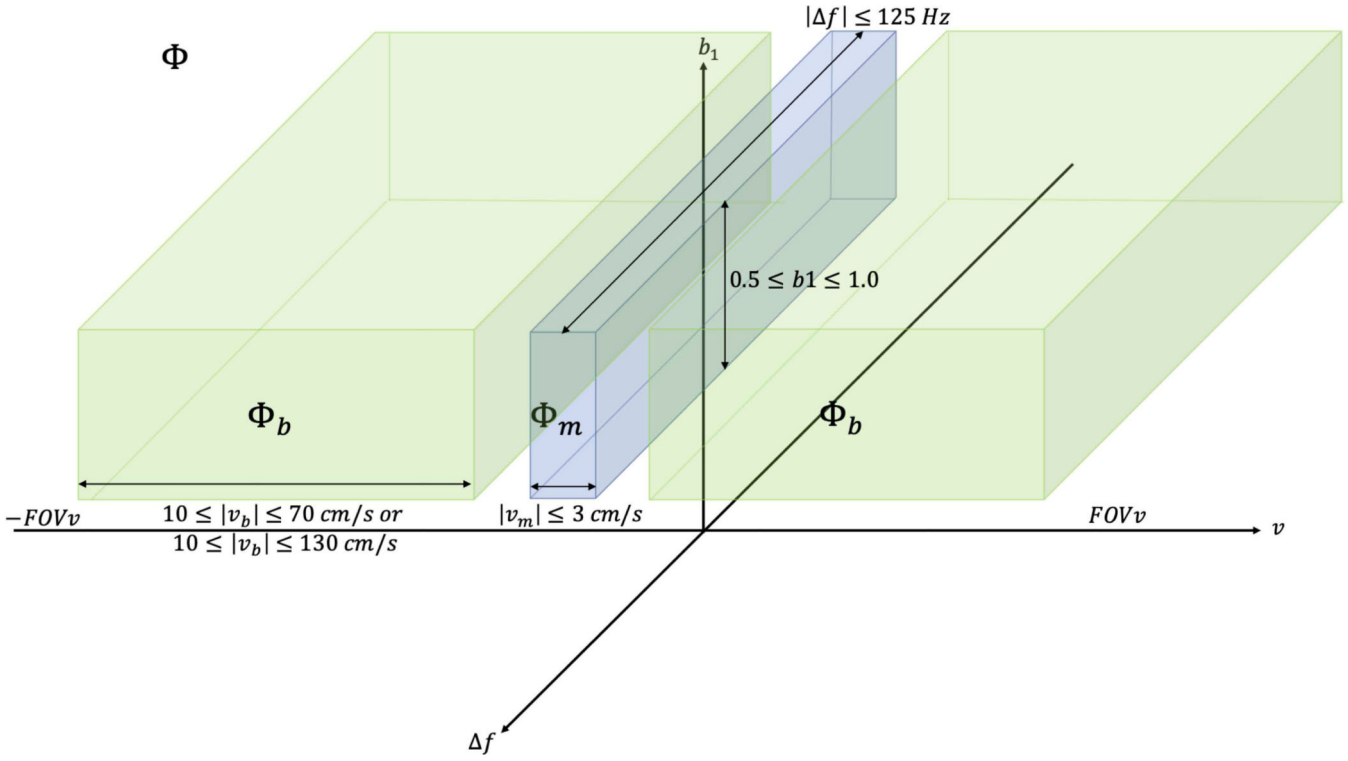

Figure 1:

Cartoon representation of Φ, which includes velocities v over ±FOV_v, off-resonance values Δf across ±125 Hz, and RF transmit scaling b_1 from 1–0.5. $\Phi_b \in \Phi$, where Φ_b includes only low-velocities v_m anticipated over the myocardium during stable diastole. $\Phi_m \in \Phi$, where Φ_m includes the range of expected coronary arterial blood velocities v_b. v represents the velocity vector component encoded along the z-direction. While this whole space is considered for optimization, later figures only show ASL signal as a function of off-resonance for b_1=1, and ASL signal as a function of b_1 scale for $\Delta f = 0$.

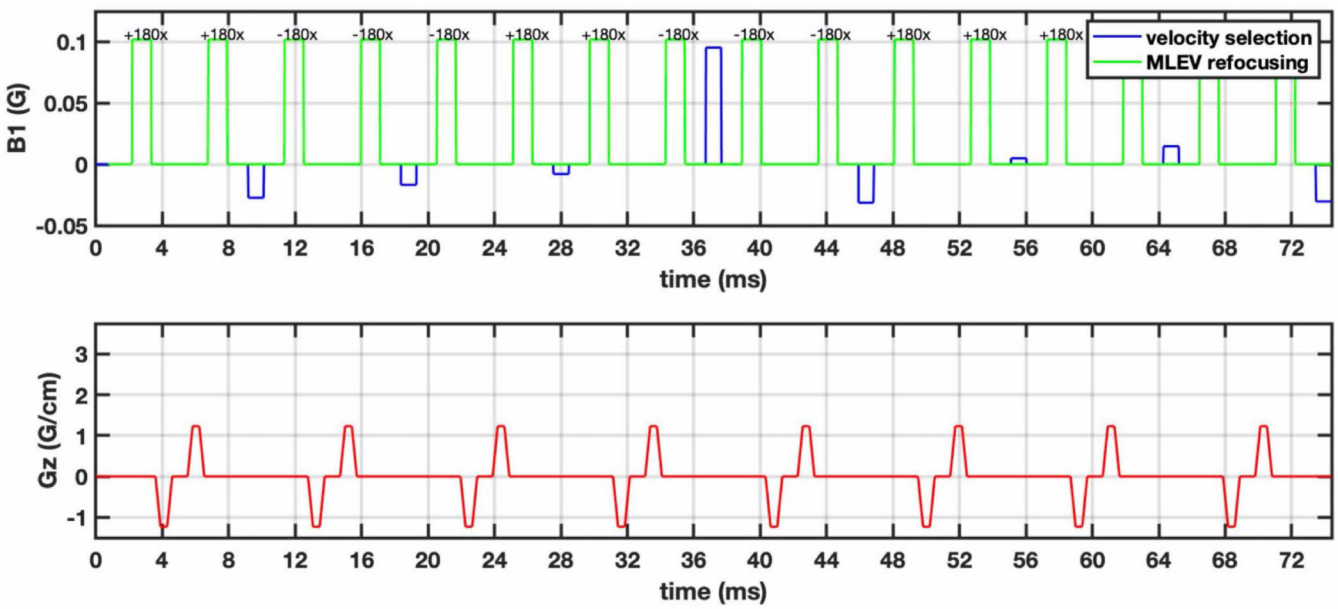

Figure 2:

The proposed VSI pulse is designed using a Fourier Transform based Velocity-Selective labeling pulse train to reduce spurious labeling of moving myocardium and achieve better labeling efficiency. This pulse is ~2x the duration of the original VS pulse and larger signal loss due to relaxation. 9 sub-pulses (blue) achieve velocity-selective inversion. Hard refocusing pulses (green) utilize MLEV phase cycling to reduce sensitivity to off-resonance. Bipolar gradients (red) between paired refocusing pulses achieve velocity encoding while removing potential for VS-stripe artifact. A 0.25 ms delay follows each gradient pair to reduce sensitivity to eddy currents.

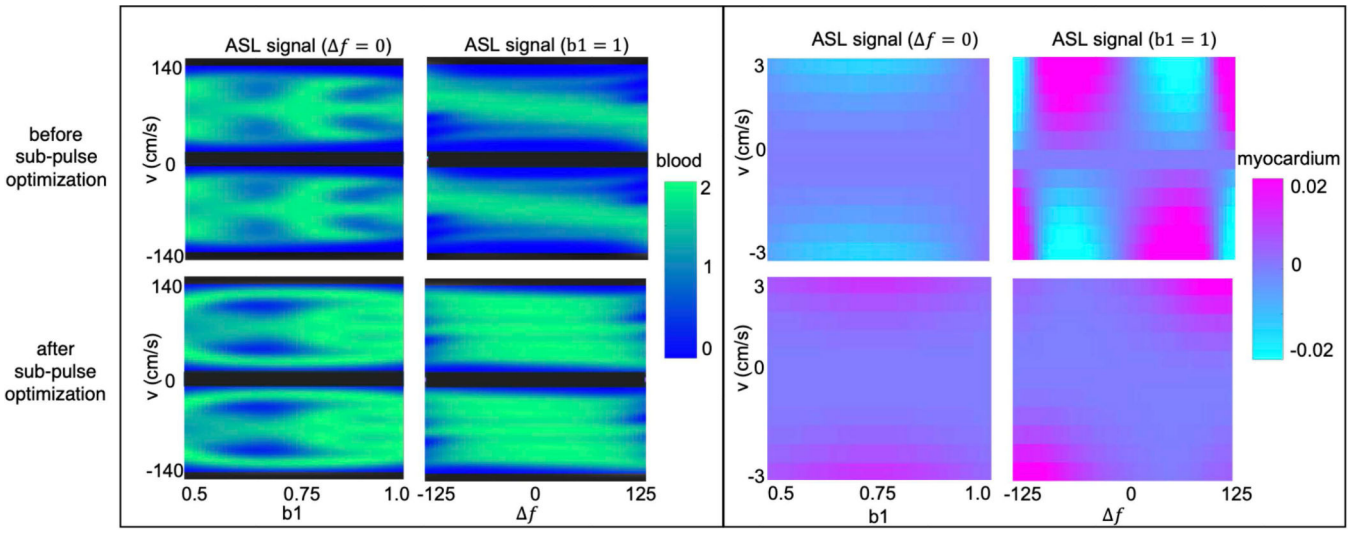

Figure 3:

Bloch simulations of the proposed VS pulse with FOV_v =140 cm/s for coronary $10 \leq |v| \leq 130\ cm/s$ (left) and for myocardial velocities $|v| \leq 3\ cm/s$ before (top) and after (bottom) optimization of sub-pulse amplitudes. Bloch simulations are shown for $\Delta f = 0$ and $b1 = 0.5 - 1$ as well as $b1 = 1$ and $|\Delta f| \leq 125\ Hz$. The VS pulse achieves better labeling efficiency of flowing signal (green regions) after optimization, especially for different off-resonance values. In addition, it can be seen that the VS pulse allows for less spurious labeling of moving myocardium (purple regions) after optimization.

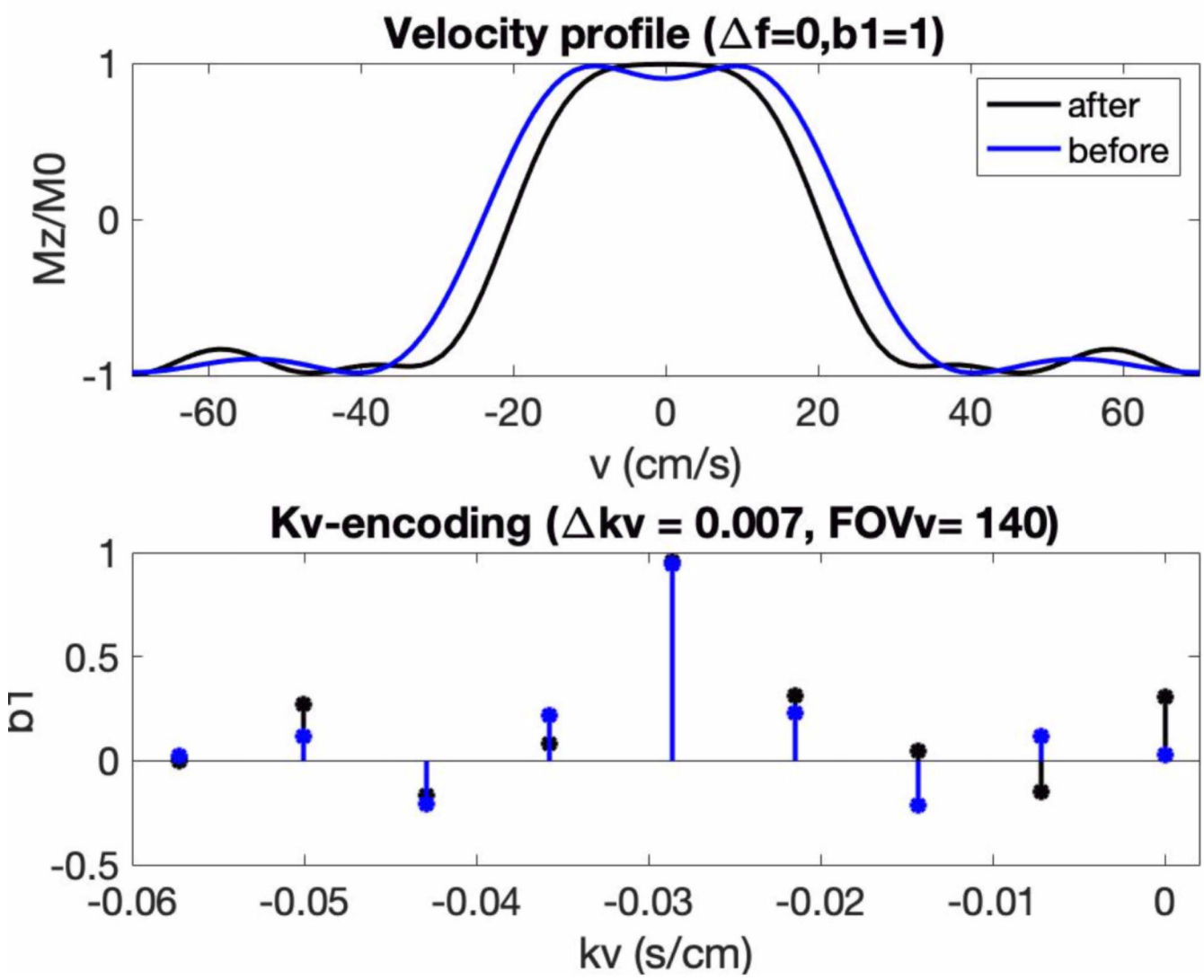

Figure 4:

On-resonant, b_1=1 velocity profile (top) and corresponding k_v-encoding (blue) for the proposed VS pulse with FOV_v=140 cm/s before (black) and after (blue) sub-pulse optimization. The k_v-encoding is shaped as a windowed sinc, which leads to a slice-like selection of velocities. After optimization, the transition band of the velocity profile narrows, improving labeling efficiency of coronary velocities above ±10 cm/s. The velocity profile also flattens around v=±3 cm/s, reducing the potential to spuriously label moving myocardium in stable diastole.

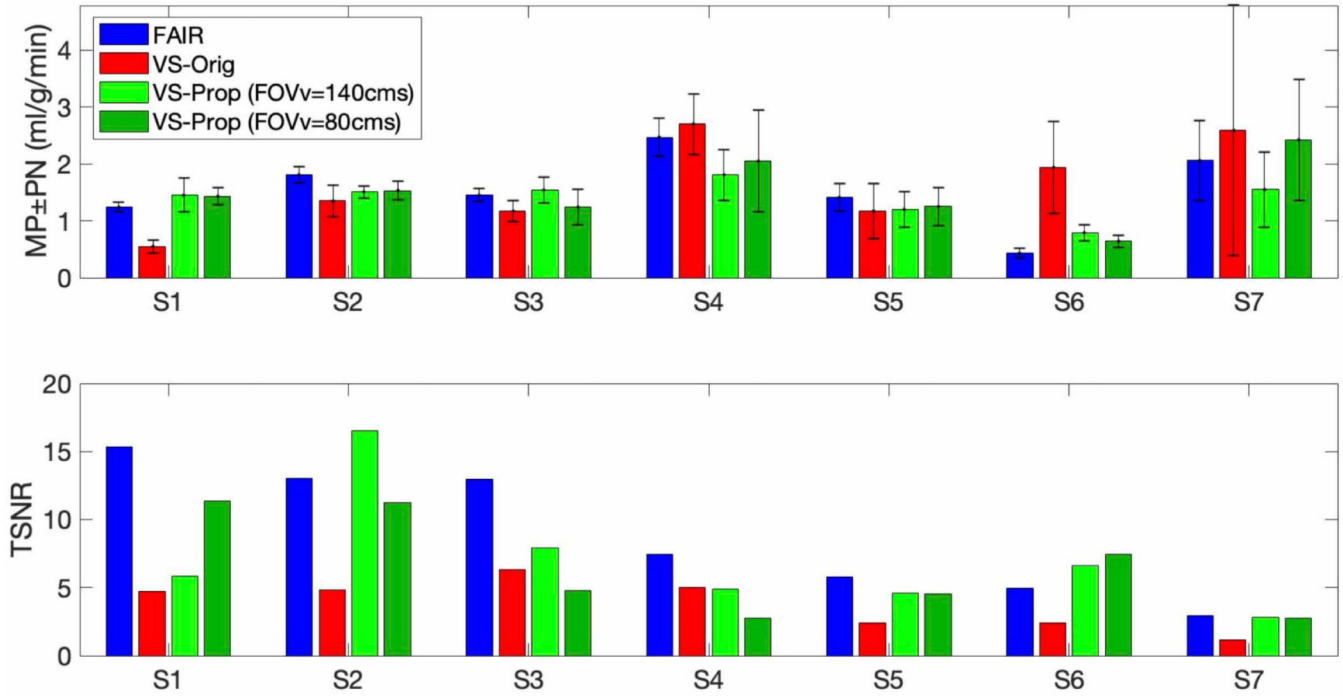

Figure 5:

Myocardial perfusion (MP), physiological noise (PN), and temporal SNR (TSNR) across seven healthy subjects (age 24–33Y, sex 3M/4F) using FAIR-ASL and VS-ASL with the original (VS-Orig) or proposed (VS-Prop) VS pulses. MP measurements between VS-Prop VS-ASL and FAIR ASL were comparable as determined by a TOST test with a difference level of 0.5 ml/g/min and p=0.05. TSNR was higher in VS-Prop VS-ASL and FAIR-ASL compared to VS-Orig VS-ASL in 5 of 7 subjects (S1, S2, S3, S6, and S7). Subjects are shown in order of decreasing FAIR TSNR (left to right).

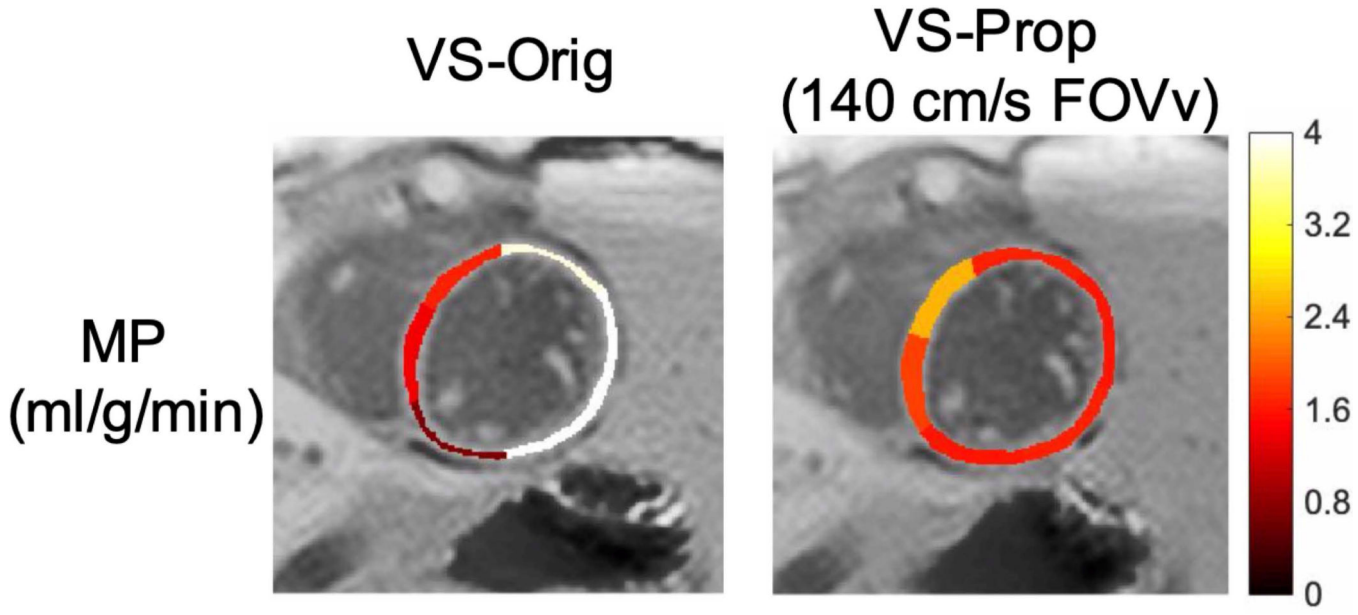

Figure 6:

Myocardial perfusion (MP) is shown in subject 1 using the original (VS-Orig) and proposed (VS-Prop) pulse. The Vs-Orig pulse has very high MP (>4 ml/g/min) in the lateral wall, indicating possible spurious labeling of moving myocardium. Comparatively, VS-prop has more consistent MP across the septal and lateral walls, indicating reduction in spurious labeling of moving myocardium.